RSC Advances

This is an *Accepted Manuscript*, which has been through the Royal Society of Chemistry peer review process and has been accepted for publication.

Accepted Manuscripts are published online shortly after acceptance, before technical editing, formatting and proof reading. Using this free service, authors can make their results available to the community, in citable form, before we publish the edited article. This *Accepted Manuscript* will be replaced by the edited, formatted and paginated article as soon as this is available.

You can find more information about *Accepted Manuscripts* in the **Information for Authors**.

Graphene oxide-based composite hydrogels with self-assembled macroporous structures

Yiwan Huang [a†], Ming Zeng [a, b, c*], Zijian Feng [a], Die Yin [a], Qingyu Xu [a], Liren Fan [a, b]

[a]*Faculty of Materials Science and Chemistry, China University of Geosciences,*

Wuhan 430074, P. R. China

[b]*Engineering Research Center of Nano-Geomaterials of Ministry of Education, China*

University of Geosciences, Wuhan 430074, P. R. China

[c]*Zhejiang Research Institute, China University of Geosciences, Wuhan 430074, P. R.*

China

[*] Corresponding author. Tel.: +86 18064129618.
E-mail address: mingzeng@cug.edu.cn, zengming318@163.com (M. Zeng).
† Present address: Graduate School of Life Science, Hokkaido University, Sapporo 060-0810, Japan (Y. Huang)

Abstract

Self-assembly technique provides a new and simple route for designing porous hydrogels. At present, most work of graphene oxide (GO)-polymer hydrogels concentrates on mechanical reinforcement. Developing a self-assembled GO-based porous hydrogel along with swelling and mechanical merits is still challenging, yet very interesting and desirable for practical applications. Herein, we report self-assembled GO-based macroporous composite hydrogels by integrating GO sheets and chitosan-based hydrogel networks. GO sheets, containing adequate hydrophilic functional groups, can be dispersed well and thereby form self-assembled supramolecular structures with polymer chains by effective intermolecular interactions (e.g., hydrogen bonding, electrostatic attraction or covalent bonding). Surprisingly, an extremely low amount (0.05–0.30 wt%) of GO can remarkably affect the architecture of hydrogel networks, leading to the formation of macroporous composite hydrogels. On the whole, the GO-based polymer composite hydrogels possess both macroporous structures (10–100 μm) and enhanced mechanical performance, yet can still hold the similar swelling properties from their parent polymeric hydrogel. Therefore, this work provides a simple route for fabricating porous hydrogels, which can probably find some potential applications in wastewater treatment or biomedical engineering system.

Introduction

Polymeric hydrogels are water-rich, crosslinked hydrophilic polymer networks.[1] They have attracted great interest all over the world in recent years, because of their promising potentials in diverse application fields, such as biological system, medical engineering, food industry, agriculture and environmental treatment.[2–6] To realize the practical applications in some fields, for example biomedical engineering system or wastewater treatment, gel scientists usually prefer to design hydrogels with porous structures for effectively accepting cells or adsorbing heavy metals as well as organic dyes.[1,6] Several strategies have been extensively utilized to fabricate porous hydrogels, including freeze-drying,[7] foaming techniques[8] and phase separation.[9]

It is worth noting that the self-assembly technique provides a new and simple route for designing porous gels. Self-assembly has been generally recognized as one of the most amazing strategies for integrating materials with unique structures or some new functions, mainly on the basis of noncovalent intermolecular interactions.[10–12] Recently, this self-assembly strategy has also been utilized to develop hydrogels or aerogels with unique porous structures from a good kind of nanoscale building blocks, graphene and its derivative graphene oxide (GO).[13–16] In fact, GO is also a unique candidate for fabricating self-assembled composite hydrogels because GO contains adequate hydrophilic groups (*i.e.*, –OH, –C–O–C–, –C=O and –COOH groups) on the surface and at the edge.[17] It is easy for GO to form an effective interfacial interaction with a hydrophilic matrix through noncovalent or covalent bonds. According to the unprecedented physical and chemical properties (*e.g.*, high surface area, high thermal conductivity, mechanical strength, and excellent electrical conductivity) of GO sheets, most work of GO-polymer hydrogels mainly

concentrates on mechanical enhancement or realizing some functions.[6,18–23] Interestingly, a self-assembled GO/poly(vinyl alcohol) hydrogel have also been prepared and shows a good pH-sensitivity, where GO acts as a 2D molecular building block.[24] Furthermore, self-assembled hydrogels from GO and DNA biomolecules have been fabricated with *in situ* formed porous structures, exhibiting a high dye-adsorption capacity.[25] However, the current work on self-assembled macroporous GO-polymer hydrogels is still limited.

Chitosan (CS), a cationic natural polysaccharide, bears abundant hydrophilic active groups (*i.e.*, –OH and –NH$_2$ groups), which can provide effective interaction sites with GO sheets, including hydrogen bonding, electrostatic attraction or covalent bonding, for self-assembly.[6,26–30] Yan et al. developed a supramolecular hydrogel by self-assembly of chitosan chains with GO sheets; yet, its mechanical strength and swelling property are not satisfied.[31] Therefore, the development of novel self-assembled porous GO-based polymeric hydrogels combined with good mechanical as well as swelling properties is considered to be a very interesting and desirable study for practical applications. It is noted that chitosan grafted polymer hydrogel occupying crosslinking networks, *e.g.*, chitosan-graft-poly(acrylic acid) (CS-*g*-PAA) hydrogel, has the advantages of the satisfied swelling and mechanical properties.[32] Thus, chitosan grafted polymer hydrogel is probably a good polymer matrix candidate for designing the novel self-assembled GO-based porous hydrogel with swelling and mechanical merits.[26,32]

In this work, we report self-assembled GO-based macroporous composite hydrogels by integrating GO sheets and CS-g-PAA polymeric networks, along with enhanced mechanical performance. In detail, the microstructure and its formation mechanism, and the intermolecular interactions of composite hydrogels are

thoroughly discussed. Their swelling capacity, salt- and pH-sensitivities, as well as mechanical performance are also evaluated. This work therefore not only provides a simple path for fabricating porous hydrogels but also gives some insight into the formation of self-assembled polymer composite hydrogels *via* effective intermolecular interactions. The self-assembled macroporous composite hydrogels combined with mechanical and swelling merits can probably find some potential applications in wastewater treatment or biomedical engineering system.

Experimental

Materials

Natural graphite flake (23 μm, 99.99% purity) was purchased from Qingdao Guyu Graphite Co., Ltd. Chitosan (CS) with a molecular weight of 900 kDa and a deacetylation degree of 85% was obtained from Sigma-Aldrich. Acrylic acid (AA) was distilled under reduced pressure prior to use. Acetic acid (HAc), sodium hydroxide (NaOH), ammonium pursulfate (APS) and *N,N′*-methylenebisacrylamide (MBAA) were of analytical grade and used as received. All solutions in the experiments were prepared with deionized water.

Preparation of GO sheets and GO/CS-*g*-PAA composite hydrogels

Graphite oxide was synthesized *via* a modified Hummers method described in our previous work.[18,33] Briefly, to generate fully exfoliated GO sheets, 0.20 g of graphite oxide powder was dispersed into 100 mL of deionized water, followed by an ultrasonic treatment for 30 min to form a stable GO solution (yellow-brown color, 2 mg/mL).

For preparing GO/CS-*g*-PAA composite hydrogels, a desired amount of GO

solution was added into 60 mL of 1% (v/v) HAc solution, followed by dissolving 1.00 g of CS powder in this solution at 20 °C. The viscosity of the mixed solution increased sharply and the solution changed into gel immediately. The gel solution was stirred overnight, and then treated by ultrasonication in an ice-water bath for 30 min to guarantee a homogenous dispersion. After that, 2 mL of 0.10 g/mL APS solution was added into the above solution with stirring at 60 °C. Ten minutes later, 7.20 g of AA and 0.20 g of MBAA were respectively added into the solution with stirring and then the reaction cell was kept at 60 °C for 2 h to complete the polymerization. The resultant products were allowed to cool down to ambient temperature and were cut into small pieces, followed by the neutralization with aqueous NaOH solution to pH 8. Then, the products were washed with deionized water until pH 7 and were dehydrated with ethanol for 24 h. After complete dehydration, the hard products were vacuum-dried at 50 °C to a constant weight for characterization. By changing the weight ratio (0.05–0.80 wt%) of GO to AA, a series of GO/CS-*g*-PAA composite hydrogels were fabricated. The pure CS-*g*-PAA hydrogel was also obtained according to the above procedure only without GO added.

Swelling properties of GO/CS-*g*-PAA composite hydrogels

The swelling ratios of dried samples in deionized water, normal saline, salt solutions and various pH (1–13) solutions were measured by a gravimetric method previously described.[18,34] The different pH values of the solutions were adjusted by using HCl and NaOH solutions, where the ionic strength was kept constant (0.1 M) by adding a desired amount of NaCl. The swelling ratios (W) of hydrogel samples were calculated by $W = (W_s - W_d) / W_d$, where W_s was the weight of swollen samples and W_d was the weight of dried samples. W was calculated as grams of water per gram of

samples. At least three measurements were carried out for each sample and the average value was calculated.

Characterizations

Fourier transform infrared (FTIR) spectra of dried samples were recorded on a Thermal Scientific Nicolet 6700 spectrometer using the KBr disk method in a wavenumber range of 4000–400 cm^{-1}. Wide-angle X-ray diffraction (WXRD) measurements were performed on a Philips X'Pert Pro MPD X-ray diffractometer using Cu Kα radiation (λ=15.405) in a diffraction angle range of 3–40 $^{\circ}$. The morphologies of the wet hydrogel samples were observed directly by using a Leica DM2500 P optical microscope (OM). The cross-section morphologies of dried hydrogel samples were obtained by using an FEI Inspect F field emission scanning electron microscope (FESEM). Thermo gravimetric analysis (TGA) and corresponding differential thermo gravimetric analysis (DTG) of dried samples were conducted at a nitrogen atmosphere with a heating rate of 10 ^{o}C min^{-1} by using a Netzsch TG 209F1 instrument in a temperature range of 25–700 ^{o}C.

Results and discussion

Formation of GO/CS-*g*-PAA composite hydrogels

To obtain homogeneous GO-polymer composite hydrogels, it is very important to not only guarantee a good dispersion of GO sheets in the pre-gel solution but also keep this dispersion stable until the hydrogel formation.[35] As presented in Figure 1a, the chemical structures of graphene oxide, chitosan and acrylic acid are sketched, respectively. The GO surface consists of sufficient hydrophilic functional groups (*i.e.*, –COOH, –C=C–, –C–O–C– and –C–OH groups), which is considered to

be very beneficial for its stable dispersion in water and also for the self-assembly by effective intermolecular interactions with hydrophilic chitosan chains. Herein, the preparation procedure of composite hydrogels is also briefly described in Figure 1b. It is expected that chitosan molecules can be well dissolved in the aqueous GO solution and then form effective interactions with GO sheets. Indeed, as we observed, when adding CS powder into the GO solution, the viscosity of this mixed solution increased sharply and the solution changed into gel immediately, directly suggesting the formation of good CS-GO combination *via* effective intermolecular interaction, *e.g.*, hydrogen bonding or electrostatic attraction. In fact, these strong interactions have already been confirmed as the driving force of self-assembly to obtain the CS/GO nanocomposite films from CS and GO in aqueous media.[27,29] The simultaneous improvement of strength and toughness of the nanocomposite films could be attributed to the homogeneous dispersion and unidirectional alignment of GO sheets in the chitosan matrix, and the strong interfacial adhesion between GO and chitosan.[27] After magnetic stirring, as shown in Figure 1c, the above CS-GO gels became to viscous CS-GO solution again, and GO sheets could be well dispersed in the chitosan solution. Then the homogeneous GO/CS-g-PAA composite hydrogels could be formed subsequently after graft polymerization of acrylic acid.

Based on the above experimental observations, the self-assembled CS-GO combination formed prior to graft polymerization. Although the combined units would be destroyed to some extent under magnetic stirring, it is supposed that the remaining CS-GO units probably affected the structure formation of composite hydrogels. Furthermore, the noncovalent intermolecular interactions between GO and CS-*g*-PAA network in the composite hydrogels would still occur based on the chemical structure characters of components. The above assumption prompts us to

explore the microstructure and its formation mechanism of composite hydrogels in the following discussion.

Microstructure and formation mechanism of GO/CS-*g*-PAA composite hydrogels

To study the microstructure and formation mechanism of GO/CS-*g*-PAA composite hydrogels, the morphologies of wet hydrogel samples were directly observed by optical microscope, as shown in Figure 2. It is interestingly found that the incorporation of GO into the CS-*g*-PAA pure hydrogel networks is beneficial for producing porous structures. The pure hydrogel exhibits a relatively dense gel network microstructure. As the amount of GO increases from 0.05 wt% to 0.30 wt%, however, the GO/CS-*g*-PAA composite hydrogels show interconnected macroporous structures, and the range of pore sizes is approximately 10–100 μm. Furthermore, with increasing the amount of GO, the pore size increases gradually and there appear parallel-aligned interconnected pores. These porous structures are very similar to the previous observation in the macroporous polyisobutylene gels.[36] This result reveals that the effective interactions between GO sheets and polymer chains do significantly affect the structure construction of hydrogel matrix.

As the amount of GO increases further (> 0.30 wt%), however, the composite hydrogels become non-porous again, which might be attributed to both the increased crosslinking density of hydrogel networks and the apparent aggregations of excessive GO sheets in the matrix. Therefore, a proper amount of GO addition can result in the formation of self-assembled macroporous structures in the composite hydrogel networks.

To briefly understand the intermolecular interactions between GO sheets and hydrogel matrix, the cross sections of vacuum-dried hydrogel samples were observed

by FESEM and the morphologies with different magnifications are presented in Figure 3. It is found that the microstructures of hydrogel samples after dewatering are quite different from the observation by optical microscope. In the FESEM observation, the CS-*g*-PAA pure hydrogel (Figure 3a) shows a relatively loose microstructure, which is intimately related to its covalent-crosslinked polymeric networks. With increasing the amount of GO, the fracture surfaces of composite hydrogels (Figure 3b–d) become compact gradually, which indicates the existence of intermolecular interactions between GO and polymer chains. Furthermore, there appears to be a parallel-aligned fracture surface in the composite hydrogel with 0.30 wt% GO loadings (Figure 3c), which might be in accordance with the parallel-aligned interconnected pores observed by optical microscope (Figure 2). The similar fracture surface was also observed and explained in the GO/chitosan nanocomposite films, where the unidirectionally aligned GO sheets were *in situ* formed in the chitosan matrix and enhanced its mechanical properties as well.[27]

WXRD is also an effective method to evaluate the exfoliation and dispersion of GO sheets in a polymer matrix by the interlayer spacing change of graphite oxide.[18,19,37] As shown in Figure S1, comparing with pristine graphite, the interlayer spacing of graphite oxide is increased from 0.336 to 0.817 nm, indicating the weakening of interlayer van der Waals forces. Furthermore, the complete disappearance of the crystalline peak of graphite oxide in the composite hydrogel suggests that the exfoliated GO sheets are well dispersed in the matrix because of the effective intermolecular interaction, which is in agreement with the FESEM observation (Figure 3).

Herein, we briefly explain the microstructure difference between pure and composite hydrogels in wet and dry states, as described in Figures 2 and 3,

respectively. For CS-*g*-PAA pure hydrogel, because of its covalent hydrogel networks, the expended polymer chains just shrink to stacked polymer chains from the wet state to the dry state, and the interactions between polymer chains are relatively weak. For GO/CS-*g*-PAA composite hydrogels, however, the intermolecular interactions (*e.g.*, hydrogen bonding or electrostatic attraction) between GO and shrunk polymer chains might be further enhanced from the wet state to the dry state, due to the existence of numerous oxygenated groups on the surface of GO sheets and the decrease of intermolecular distance. Thus, the composite hydrogels become much denser than the pure one after dewatering, as observed by FESEM in Figure 3.

Additionally, we also attempt to discuss the possible formation mechanism of the self-assembled macroporous composite hydrogels. As we mentioned previously, when dissolving chitosan into GO solution, the CS-GO combinations were self-assembled due to the effective intermolecular interactions. Because of the existence of adequate active –NH$_2$ groups in the CS-GO units, it is easy for the monomer AA (containing an active –C=C– group) to be covalently grafted onto CS molecular chains, which will be further confirmed by the FTIR result in the following discussion (Figure 4a). After graft polymerization, it is assumed that the composite hydrogels would exhibit relatively dense networks at the local zone of CS-GO unit and relatively loose networks at the far zone of this unit. As shown in Figure 2c (left), when the amount of GO is relatively low (< 0.15 wt%), the porous hydrogels with relatively small pore sizes can be dominated by this active CS-GO unit. With increasing the amount of GO a little bit higher (0.15–0.30 wt%), the active CS-GO unit tends to form a bigger and relatively uniform "porous unit" (revealed in Figure 2c, right) with surrounding polymer chains. As a result, the porous hydrogels show relatively larger and homogeneous pore size distribution.

Therefore, GO/CS-*g*-PAA composite hydrogels with self-assembled macroporous structures were synthesized successfully by a facile strategy of *in situ* radical polymerization in this study, which provides a novel route for fabricating porous hydrogels. Based on the CS-GO combination units, the covalent and noncovalent intermolecular interactions between GO and CS-*g*-PAA polymer networks would further occur to form the macroscopic-assembled composite hydrogels, which should be emphasized here.

Intermolecular interactions between GO and CS-*g*-PAA

The FTIR spectra of GO, CS, CS-*g*-PAA hydrogel and GO/CS-*g*-PAA composite hydrogels are shown in Figure 4a. In the spectrum of GO, the absorption peaks at 1724, 1615, 1225 and 1060 cm^{-1} are the characteristics of –COOH, –C=C–, –C–O–C– and –C–OH groups respectively, which is in good agreement with the previous studies,[18,19] and proves the successful oxidation from graphite to graphite oxide. In the spectrum of CS, the absorption peaks at 1655, 1596 and 1060 cm^{-1} are related to the vibration of –C=O (–NHCO–), –NH$_2$ and –C–OH groups respectively.

After graft polymerization, in the spectrum of CS-*g*-PAA hydrogel, the peak of –NH$_2$ groups at 1596 cm^{-1} disappears, and the peaks of –C=O (–NHCO–) and –C–OH groups at 1655 and 1060 cm^{-1} respectively become weak. Meanwhile, the absorption peaks at 1545 and 1403 cm^{-1} corresponding to the characteristics of –COO$^-$ groups appear, indicating that the monomer AA has covalently grafted onto CS molecular chains successfully. Furthermore, the intermolecular interactions between GO and CS-based polymer hydrogels are important for the self-assembled supramolecular structures and properties of GO/CS-*g*-PAA composite hydrogels. Compared to the spectrum of CS-*g*-PAA pure hydrogel, some absorption peaks change in intensity or

even disappear, and some new absorption peaks appear in the spectra of GO/CS-*g*-PAA composite hydrogels, revealing the existence of effective intermolecular interactions between GO and polymer chains. As the amount of GO increases, the absorption peak of –COO⁻ groups at 1545 cm⁻¹ becomes broad visibly, and two shoulder peaks even appear at around 1545 cm⁻¹ (for 0.10 and 0.80 wt% GO-gels), demonstrating that hydrogen bonds exist between GO and polymer networks. In addition, in the spectra of composite hydrogels, the absorption peak at 1724 cm⁻¹ related to –COOH groups of GO disappears, and the characteristic peak of pure hydrogel at 1445 cm⁻¹ becomes weak gradually and even disappears with further increasing the GO loadings. These evidences suggest that covalent bonds might form between the –COOH groups of GO and the active groups (e.g. $-NH_2$ or –OH groups) of polymer networks. In fact, the reaction between GO and polymers has also occurred in other GO/polymer composites.[18,19,38] Therefore, as schematically demonstrated in Figure 1b (right), the self-assembled supramolecular structures *via* effective covalent and noncovalent intermolecular interactions are probably formed in these GO-based composite hydrogels.

It has been reported that the effective interactions can enhance the thermal property of polymers even with a very low amount of GO added.[18,33,38] As shown in Figure 4b and c, the thermal behavior of vacuum-dried CS-*g*-PAA hydrogel and GO/CS-*g*-PAA composite hydrogels was evaluated by TG and DTG methods. Both pure and composite hydrogels decomposed mainly in a two-step process, and the composite hydrogels exhibit a mildly enhanced thermal property in the temperature range of 375–500 °C, compared to that of the pure one.

The first step of the weight loss from 30 to 375 °C was mainly attributed to the dewatering of the freezing-bonded and bonded water molecules, as well as the

decomposition of the oxygenated functional groups in the hydrogel networks.[16,21,22,39] From the TG curve of graphene oxide (Figure S2), it is easy to understand that the weight loss of composite hydrogels is a little bit larger than that of pure hydrogel in this step mainly because of the introduction of numerous oxygenated hydrophilic groups by GO sheets. The second step of the weight loss from 375 to 500 °C was related to the thermal decomposition of hydrogel networks. The parameters of the thermal decomposition behavior of pure and composite hydrogels, including the initial decomposition temperature (T_i), the temperature with maximum decomposition rate (T_{max}), the final decomposition temperature (T_f) and the maximum decomposition rate (V_{dec}) are also listed in Table S1. It can be found that the addition of a very low amount ($\leq$ 0.50 wt%) of GO can improve the thermal property of dried hydrogels to some extent. In detail, the T_i, T_{max} and T_f of the composite hydrogel with 0.10 wt% GO loadings appear at 417.7, 429.1 and 470.9 °C, and are increased by 4.0, 1.0 and 3.8 °C respectively, as compared to the pure hydrogel. In addition, the values of V_{dec} and the weight loss of this composite hydrogel are 4.58 % min^{-1} and 21.80 % respectively, which are slightly lower than that of the pure one. This enhancement of thermal property is also due to the fact that the active GO sheets can form effective intermolecular interactions with the polymer matrix, which has been confirmed by FESEM and FTIR results shown in Figures 3 and 4a. Further, the addition of GO might also increase the crosslinking density of hydrogel networks, resulting in an enhanced thermal property of composite hydrogel. When the amount of GO was increased from 0.10 wt% to 0.50 wt%, however, the thermal property of composite hydrogel was not improved obviously, probably because the partial aggregations of GO in the polymer networks are not beneficial for the improvement of thermal property.

Thereby, the above FTIR, TG and DTG results further demonstrate that the effective intermolecular interactions exist between GO sheets and polymeric networks, which are considered to be crucial for the formation of self-assembled macroporous composite hydrogels.

Swelling and mechanical properties of GO/CS-*g*-PAA composite hydrogels

From the above discussion, it is clear that GO sheets can form interactions with the polymeric hydrogel networks through noncovalent and covalent bonding, and can significantly influence the microstructures of hydrogels as well. The incorporation of GO might also affect the swelling capacities of hydrogels. Meanwhile, the evaluation of the swelling capacities of hydrogels in aqueous solutions is critically essential for both fundamental understanding and practical applications. As shown in Figure 5a, the swelling ratios of both pure and composite hydrogels in normal saline decline sharply compared to that in deionized water. Despite the existence of self-assembled structure due to the introduction of GO sheets, the composite hydrogels are mainly structured by covalent bonds and hydrogen bonds, as illustrated in Figure 2b. Therefore, the above significant difference of composite hydrogels in swelling ratios between in water and in normal saline can still be explained as a common phenomenon in the swelling of polyelectrolyte hydrogels.[18,34] This phenomenon is due to the fact that the charge screening effect of counter-ions (Na^+ or Cl^-) on the charged groups ($-COO^-$ or $-NH_3^+$) in the hydrogel networks can induce a clear decline of electrostatic repulsions, resulting in a decrease of the osmotic pressure between hydrogel networks and external solution.

Several aspects might affect the swelling ratios of GO/CS-*g*-PAA composite hydrogels, such as the intermolecular interactions between the components, the

abundant hydrophilic groups on the surface of GO, the microstructures of hydrogels, and the dispersion of GO in the matrix. It can be found that the hydrogels exhibit a similar swelling tendency in two media with increasing the amount of GO. Comparing with the pure hydrogel, the swelling ratios of composite hydrogel with 0.05 wt% GO loadings decrease mildly, indicating that the intermolecular interactions between the components restrict the swelling of hydrogel networks. When increasing the amount of GO from 0.05 to 0.10 wt%, the composite hydrogels acquire evidently increased swelling ratios. The enhanced swelling capacities might be due to the influence of GO, which containing numerous hydrophilic groups can remarkably increase the density of hydrophilic groups in the hydrogel networks. Furthermore, GO sheets dispersed homogeneously in the matrix can probably improve the swelling capacities as well. However, with further increasing the amount of GO, the swelling ratios of composite hydrogels decrease apparently. This might be attributed to the further increased crosslinking density of composite hydrogel networks and the aggregations of excessive GO sheets in the matrix, which has been confirmed by the FESEM morphologies shown in Figure 3.

According to Flory's swelling theory,[40] the swelling behaviors of hydrogels are strongly affected by the ionic strength of external solutions. Additionally, the prepared hydrogels might also exhibit different swelling behaviors in a wide range of pH values since both pure and composite hydrogels contain charged groups (–COOH and –NH$_2$ groups), usually called polyelectrolyte hydrogels. As shown in Figure 5b and c, the effects of salt concentration and pH value of the media on the swelling ratios of hydrogels are presented and discussed as follows. It can be observed that both pure and composite hydrogels show a similar swelling tendency in salt and pH solutions respectively, indicating that GO sheets have very little influence on the salt-

and pH-sensitive behaviors of hydrogel networks.

As we mentioned, the swelling decline of polyelectrolyte hydrogels in salt solutions is often attributed to a charge screening effect of counter-ions, which can significantly weaken the ion-ion electrostatic repulsion among the hydrogel networks.[18,34] The effects of salt concentration on the swelling ratios of hydrogels, evaluated in NaCl solutions, are shown in Figure 5b. The swelling ratios of hydrogels decrease with increasing the salt concentration of NaCl solution due to the increased charge screening effect of counter-ions and the decreased osmotic pressure between hydrogel networks and external solution, in good accord with Donnan equilibrium theory.

From the swelling ratios of hydrogels in pH solutions (Figure 5c), it can be seen that all hydrogels exhibit a clear pH-sensitive swelling capability. It is noted that most $-NH_2$ groups on chitosan chains have been reacted and thereby consumed by the graft polymerization. Therefore, the variation in the swelling capability is mainly attributed to the changes in the protonation of the carboxylic groups on PAA chains according to the pH variations. All hydrogels acquire relatively low swelling ratios at very acidic media (pH < 3) due to the strong protonation of –COOH groups in the hydrogel networks. In this case, a great number of hydrogen bonds formed among –COOH, –OH, and –C=O groups greatly restrict the swelling of the hydrogel despite the existence of slight NH_3^+-NH_3^+ electrostatic repulsion in the hydrogel networks, leading to the relatively low swelling ratios. As the pH value of buffer solution increases, the swelling ratios of the hydrogels increase sharply and then keep a relatively stable value. This phenomenon results from the fact that numerous –COOH groups in the hydrogel networks are ionized and converted into $–COO^-$ groups, so that many hydrogen bonds are broken and the sufficient COO^--COO^- electrostatic repulsion

increases remarkably among the hydrogel networks. This effect causes the hydrogel matrix to expand, and the amount of liquid absorbed increases considerably. The above result of swelling behavior in different pH solutions is well in agreement with the previous study on chitosan-graft-poly(acrylic acid) hydrogels.[41] Meanwhile, when the amount of GO increases to 0.30 wt% and 0.50 wt%, the swelling ratios of composite hydrogels decrease slightly in both the salt and pH solutions compared to that of the pure one. This result might be also owing to the facts that the enhanced interactions between GO and polymer chains and the aggregation of GO in the matrix do not benefit the swelling of hydrogel networks.

From the above discussion, the addition of GO sheets only shows mild effects on the swelling behaviors in aqueous fluids. However, GO sheets can evidently enhance the mechanical property of composite hydrogels. As shown in Figure 6, the compressive performance of the wet composite hydrogel with 0.50 wt% GO loadings exhibits a significant reinforcement compared to that of the pure one. The pure hydrogel is very brittle and easily destroyed under a compressive load. Despite high water content ($C_W > 98$ wt%, similar to the pure hydrogel, as presented in Figure S3), the composite hydrogels are relatively tough, and only show a very small strain under a constant load. It is noted that the composite hydrogels can recover to their original shapes immediately after removing the load. This reinforcement is mainly attributed to both the unique mechanical nature of GO sheets and the intermolecular interactions between GO and polymer chains, which are beneficial for the effective load transfer in the hydrogel networks, leading to the enhanced load-bearing ability. In fact, the similar mechanical reinforcement has also been evidenced in other GO/polymer composite hydrogel systems.[19,37]

Therefore, the GO/CS-*g*-PAA composite hydrogels possess both macroporous

structures and enhanced mechanical performance, yet can still hold the similar swelling properties from their parent CS-*g*-PAA hydrogel. The composite hydrogels with these combined properties will probably demonstrate enhanced adsorption capability to heavy metal ions or organic dyes in wastewater treatments. Of course, the nature and practical applications of the porous structures for GO-based composite hydrogels requires further investigations.

Conclusions

To conclude, we have developed a series of self-assembled GO/CS-*g*-PAA macroporous composite hydrogels *via* a facile radical polymerization. Due to adequate hydrophilic oxygenated groups on the surface, GO sheets can be dispersed well and form self-assembled supramolecular structures with polymer chains by effective intermolecular interactions, such as hydrogen bonding, electrostatic attraction or covalent bonding. An extremely low amount (0.05–0.30 wt%) of GO can remarkably affect the architecture of CS-*g*-PAA hydrogel networks, leading to the formation of macroporous composite hydrogels. The self-assembled graphene oxide-chitosan units are assumed to play a critical role in the structure formation of composite hydrogels. It is worth noting that this work provides a simple path for fabricating porous hydrogels. In addition, the addition of GO sheets yet shows a slight influence on the swelling behaviors of hydrogels in various media, and the composite hydrogels exhibit salt- and pH-sensitivities, similar to the pure one. Thanks to the effective intermolecular interactions between GO and the hydrogel matrix, the composite hydrogels also demonstrate evidently enhanced mechanical performance, as compared to that of the pure hydrogel matrix. Thus, the self-assembled macroporous composite hydrogels can probably find some potential applications in

wastewater treatment or biomedical engineering system. Our coming work is going to focus on the comprehensive characterization of the mechanical properties of composite hydrogels and experiments for their practical applications.

Acknowledgements

Supporting information

The WXRD data of GO-based composite hydrogels (Figure S1), TG data of graphene oxide (Figure S2), and TG/DTG data (Table S1) and water content (Figure S3) of pure hydrogel and GO-based composite hydrogels can be found in this supporting information.

Notes and references

1   T. R. Hoare and D. S. Kohane, *Polymer*, 2008, **49**, 1993–2007.

2   J. Kopeček, *Biomaterials*, 2007, **28**, 5185–5192.

3   Kuen Yong Lee and David J. Mooney, *Chemical Reviews*, 2001, **101**, 1869–1879.

4   A. Gregorova, N. Saha, T. Kitano and P. Saha, *Carbohydrate Polymers*, 2015, **117**, 559–568.

5   M. a Zwieniecki, P. J. Melcher and N. M. Michele Holbrook, *Science (New York, N.Y.)*, 2001, **291**, 1059–1062.

6   Y. Chen, L. Chen, H. Bai and L. Li, *Journal of Materials Chemistry A*, 2013, **1**, 1992.

7   N. Kato and S. H. Gehrke, *Colloids and Surfaces B: Biointerfaces*, 2004, **38**, 191–196.

8   A. Barbetta, G. Rizzitelli, R. Bedini, R. Pecci and M. Dentini, *Soft Matter*, 2010, **6**, 1785.

9   V. Gopishetty, I. Tokarev and S. Minko, *Journal of Materials Chemistry*, 2012, **22**, 19482.

10   A. Harada, R. Kobayashi, Y. Takashima, A. Hashidzume and H. Yamaguchi, *Nature chemistry*, 2011, **3**, 34–37.

11   H. Park, A. Afzali, S.-J. Han, G. S. Tulevski, A. D. Franklin, J. Tersoff, J. B. Hannon and W. Haensch, *Nature Nanotechnology*, 2012, **7**, 787–791.

12   A. Hernandez-Garcia, D. J. Kraft, A. F. J. Janssen, P. H. H. Bomans, N. a. J. M. Sommerdijk, D. M. E. Thies-Weesie, M. E. Favretto, R. Brock, F. a. de Wolf, M. W. T. Werten, P. van der Schoot, M. C. Stuart and R. de Vries, *Nature Nanotechnology*, 2014, **9**, 698–702.

13   Y. Xu, K. Sheng, C. Li and G. Shi, *ACS Nano*, 2010, **4**, 4324–4330.

14   H. Sun, Z. Xu and C. Gao, *Advanced Materials*, 2013, **25**, 2554–2560.

15   W. Chen and L. Yan, *Nanoscale*, 2011, **3**, 3132–3137.

16   W. Ai, Z.-Z. Du, J.-Q. Liu, F. Zhao, M.-D. Yi, L.-H. Xie, N.-E. Shi, Y.-W. Ma, Y. Qian, Q.-L. Fan, T. Yu and W. Huang, *RSC Advances*, 2012, 12204–12209.

17   D. R. Dreyer, S. Park, C. W. Bielawski and R. S. Ruoff, *Chemisty Society Review*, 2010, **39**, 228–240.

18   Y. Huang, M. Zeng, J. Ren, J. Wang, L. Fan and Q. Xu, *Colloids and Surfaces A: Physicochemical and Engineering Aspects*, 2012, **401**, 97–106.

19   H. P. Cong, P. Wang and S. H. Yu, *Chemistry of Materials*, 2013, **25**, 3357–3362.

20   A. Pourjavadi, M. Nazari and S. H. Hosseini, *RSC Advances*, 2015, **5**, 32263–32271.

21   H. Zhang, X. Pang and Y. Qi, *RSC Advances*, 2015.

22   H. Zhang, D. Zhai and Y. He, *RSC Advances*, 2014, **4**, 44600–44609.

23   Y. Wang, P. Zhang, C. F. Liu and C. Z. Huang, *RSC Advances*, 2013, **3**, 9240.

24   H. Bai, C. Li, X. Wang and G. Shi, *Chemical Communications*, 2010, **46**, 2376.

25   Y. Xu, Q. Wu, Y. Sun, H. Bai and G. Shi, *ACS Nano*, 2010, **4**, 7358–7362.

26   M. Rinaudo, *Progress in Polymer Science*, 2006, **31**, 603–632.

27   Y. Pan, T. Wu, H. Bao and L. Li, *Carbohydrate Polymers*, 2011, **83**, 1908–1915.

28   G. Z. Kyzas, D. N. Bikiaris, M. Seredych, T. J. Bandosz and E. a. Deliyanni, *Bioresource Technology*, 2014, **152**, 399–406.

29   X. Yang, Y. Tu, L. Li, S. Shang and X. M. Tao, *ACS Applied Materials and Interfaces*, 2010, **2**, 1707–1713.

30   A. Ray Chowdhuri, S. Tripathy, S. Chandra, S. Roy and S. K. Sahu, *RSC Advances*, 2015, **5**, 49420–49428.

31   D. Han and L. Yan, *ACS Sustainable Chemistry and Engineering*, 2014, **2**, 296–300.

32   G. R. Mahdavinia, a. Pourjavadi, H. Hosseinzadeh and M. J. Zohuriaan, *European Polymer Journal*, 2004, **40**, 1399–1407.

33   M. Zeng, J. Wang, R. Li, J. Liu, W. Chen, Q. Xu and Y. Gu, *Polymer (United Kingdom)*, 2013, **54**, 3107–3116.

34   C. Chang, M. He, J. Zhou and L. Zhang, *Macromolecules*, 2011, **44**, 1642–1648.

35   S. Bhattacharyya, S. Guillot, H. Dabboue, J. F. Tranchant and J. P. Salvetat, *Biomacromolecules*, 2008, **9**, 505–509.

36   D. Ceylan and O. Okay, *Macromolecules*, 2007, **40**, 8742–8749.

37   L. Zhang, Z. Wang, C. Xu, Y. Li, J. Gao, W. Wang and Y. Liu, *Journal of Materials Chemistry*, 2011, **21**, 10399.

38   S. Sun and P. Wu, *Journal of Materials Chemistry*, 2011, **21**, 4095.

39   Z. X. Tai, J. Yang, Y. Y. Qi, X. B. Yan and Q. J. Xue, *RSC Advances*, 2013, **3**, 12751–12757.

40   P. J. Flory, *Principles of polymer chemistry*, 1953, 1–672.

41   F. H. A. Rodrigues, A. G. B. Pereira, A. R. Fajardo and E. C. Muniz, *Journal of Applied Polymer Science*, 2013, **128**, 3480–3489.

Figures and figure captions:
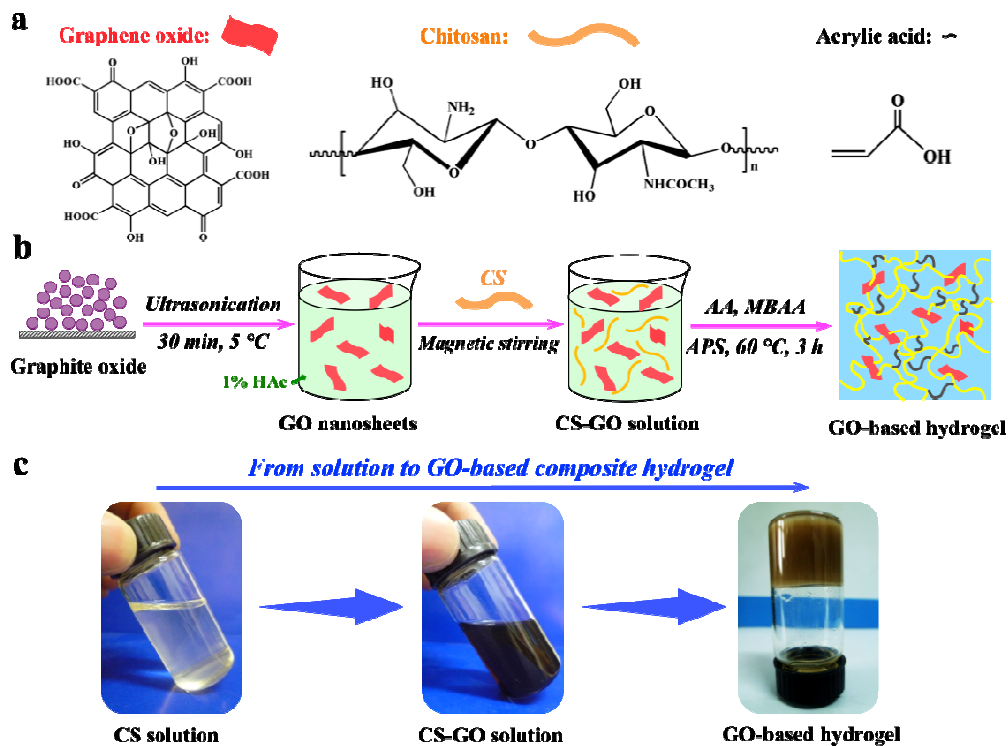
**Figure 1. Chemical structures and formation of GO-based composite hydrogels:**
(a) Molecular structures of GO, CS and AA. (b) Preparation procedure of GO-based composite hydrogels. (c) Photographs of CS solution, CS-GO mixed solution and the resultant GO/CS-g-PAA composite hydrogels.
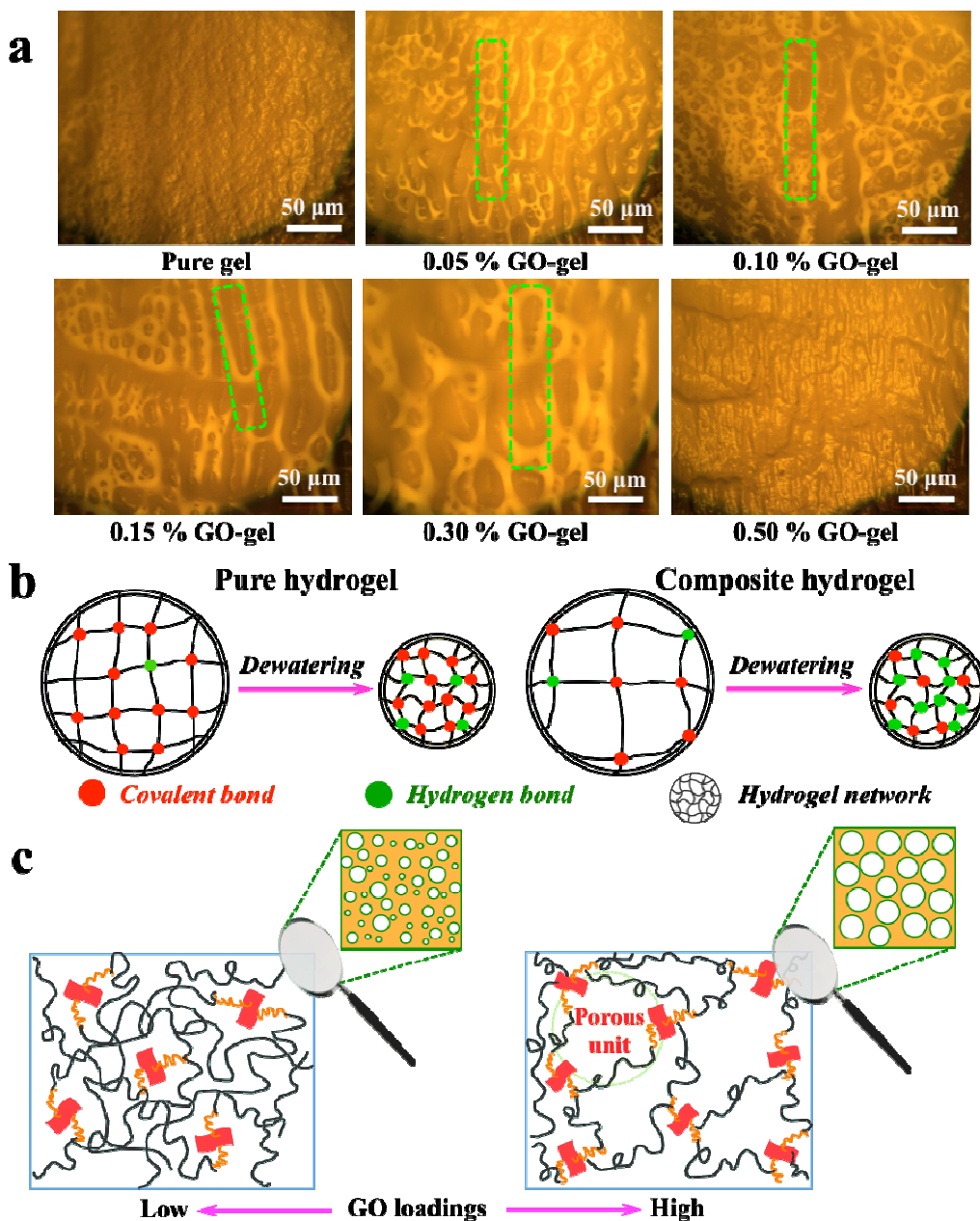
Figure 2. Self-assembled porous structures and possible formation mechanism of GO-based composite hydrogels: (a) Optical microscope images of pure hydrogel and composite hydrogels with different GO loadings in the wet state. (b) Schematic illustration of the microstructure changes of pure hydrogel and composite hydrogels from the wet state to the dry state. (c) Possible microstructures of composite hydrogels with relatively low and high GO loadings.
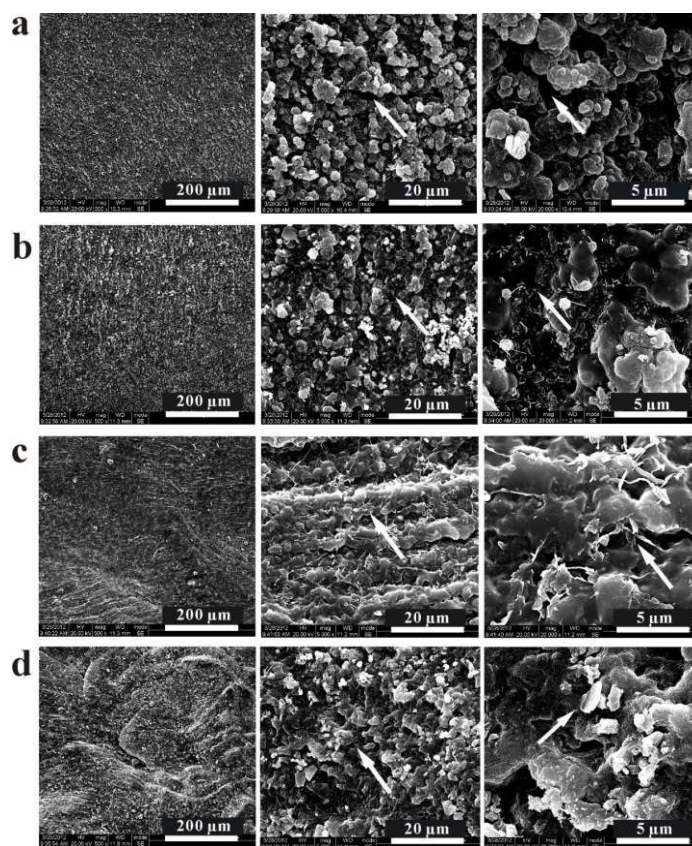
Figure 3. FESEM images with different magnifications of pure hydrogel (a) and composite hydrogels with 0.10 (b), 0.30 (c), and 0.50 (d) wt% GO loadings in the dry state.
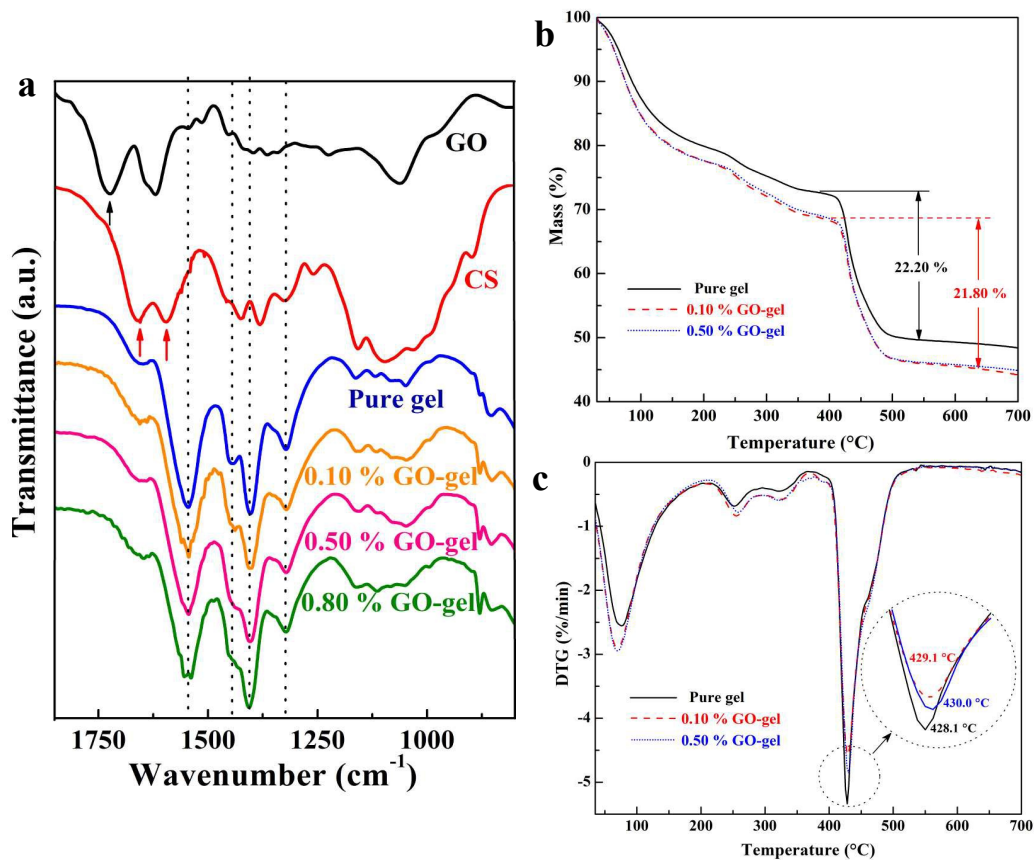
Figure 4. Characterizations of the intermolecular interactions between GO sheets and polymeric hydrogel: (a) FTIR spectra of GO, CS, pure hydrogel and composite hydrogels with different GO loadings. (b) TGA and (c) DTG curves of pure hydrogel and composite hydrogels with different GO loadings in the dry state.
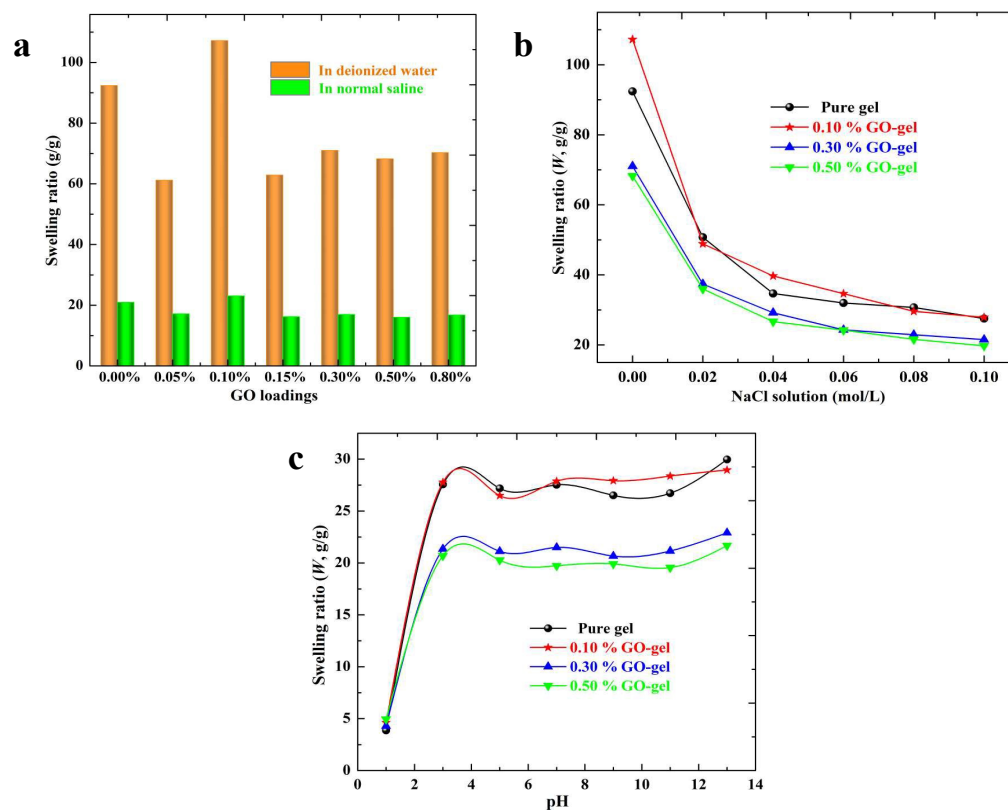
Figure 5. Swelling behaviors of GO-based composite hydrogels in various media:
(a) Swelling ratios of pure hydrogel and composite hydrogels with different GO
loadings. (b) Effects of salt concentrations and (c) pH of the buffer solutions on the
swelling ratios of pure hydrogel and composite hydrogels with different GO loadings.
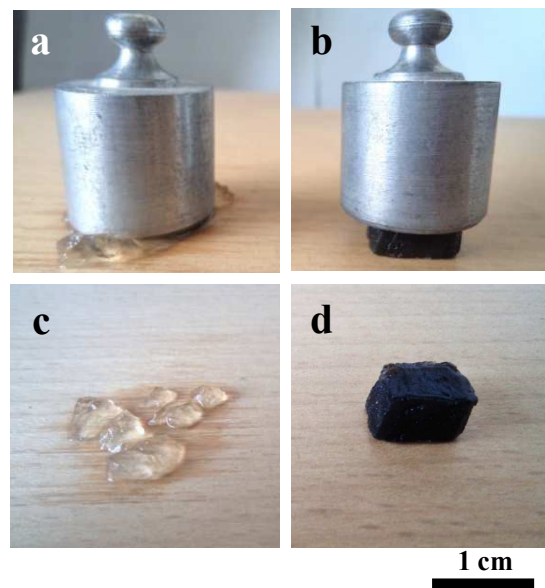
Figure 6. Photographs of pure hydrogel (a, c) and composite hydrogel (b, d) during and after compressed condition. The weight of load is 100 g.